PROCEEDINGS OF SCIENCE

Staggered rooting and unphysical phases at finite baryon density

Szabolcs Borsányi,[a] **Zoltán Fodor,**[a,b,c,e,f] **Matteo Giordano,**[c] **Jana N. Guenther,**[a] **Sándor D. Katz,**[c] **Attila Pásztor**[c,d] **and Chik Him Wong**[a,*]

[a] *Department of Physics, Wuppertal University, Gaussstr. 20, D-42119, Wuppertal, Germany*
[b] *Pennsylvania State University,Department of Physics, State College, PA 16801, USA*
[c] *Institute for Theoretical Physics, ELTE Eötvös Loránd University, Pázmány P. sétány 1/A, H-1117 Budapest, Hungary*
[d] *HUN-REN-ELTE Theoretical Physics Research Group, Pázmány Péter sétány 1/A,1117 Budapest, Hungary*
[e] *Jülich Supercomputing Centre, Forschungszentrum Jülich, D-52425 Jülich, Germany*
[f] *Physics Department, UCSD, San Diego, CA 92093, USA*

Research on the QCD phase diagram with lattice field theory methods is dominated by the use of rooted staggered fermions, as they are the computationally cheapest discretization available. We show that rooted staggered fermions at a nonzero baryochemical potential μ_B predict a sharp rise in the baryon density at low temperatures and $\mu_B \gtrsim 3m_\pi/2$, where m_π is the Goldstone pion mass. We elucidate the nature of the non-analyticity behind this sharp rise in the density by a comparison of reweighting results with a Taylor expansion of high order. While at first sight this non-analytic behavior becomes apparent at the same position where the pion condensation transition takes place in the phase-quenched theory, but the nature of the non-analyticity in the two theories appears to be quite different: While at nonzero isospin density the data are consistent with a genuine thermodynamic (branch-point) singularity, the results at nonzero baryon density point to an essential singularity at $\mu_B = 0$. The effect is absent for four flavors of degenerate quarks, where rooting is not used. For the two-flavor case, we show numerical evidence that the magnitude of the effect diminishes on finer lattices. We discuss the implications of this technical complication on future studies of the QCD phase diagram. This work is based on our publication [1].

The 40th International Symposium on Lattice Field Theory (Lattice 2023)
July 31st - August 4th, 2023
Fermi National Accelerator Laboratory

*Speaker

PoS(LATTICE2023)166

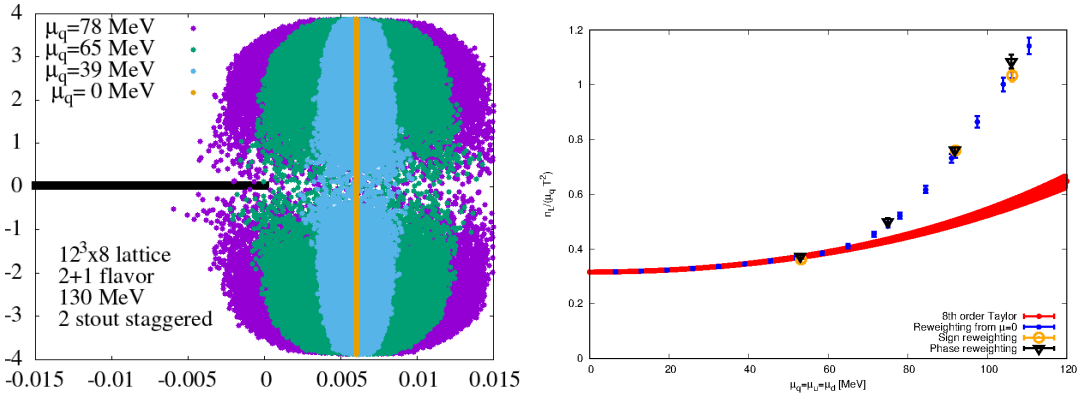

Figure 1: Left: Illustration of the Dirac spectrum at finite baryo-chemical potential. The spectrum, obtained with dense linear algebra, is based on one dynamical staggered lattice configuration of size $12^3 \times 8$ with $m_\pi = 135$ MeV, using the 2stout action. The thick line shows the standard choice for the branch cut of the complex square root. Right: A rapid rise in the light-quark density-to-chemical potential ratio as a function of μ_q around $\mu_q = m_\pi/2$ with rooted staggered fermions. Results were obtained with a lattice size of $16^3 \times 8$. We use physical quark masses, using a tree-level improved gauge action and 2 steps of stout smearing with smearing parameter $\rho = 0.15$ applied to the links entering the staggered Dirac operator, which we will call the 2stout action from now on. To better see the onset of this sharp increase, we also show the 8th-order Taylor expansion, as a smooth baseline. Different reweighting schemes agree with one another. The Taylor expansions around $\mu_q = 0$ are computed using the reduced matrix formalism [6], without employing stochastic estimators.

1. Introduction

The determination of the phase diagram of QCD on the temperature (T) – baryochemical potential (μ_B) plane with first-principle lattice QCD calculations has been an unsolved problem for decades due to the complex action problem. Several workarounds have been proposed and utilized to obtain information at nonzero μ_B. Examples include a Taylor expansion around $\mu_B = 0$, analytic continuation from imaginary chemical potentials, and different reweighting techniques. Details can be found in literature reviews, e.g. Ref. [2]. Rooted staggered fermions are the most popular fermion discretization in the literature for being the most computationally efficient. However, the theoretical justification of the application of rooted staggered fermions at finite chemical potential is not fully settled [3, 4]. Since the staggered determinant is complex at real chemical potential, one must find a way to resolve the sign ambiguity in the complex square root function. The problems caused by such ambiguity are expected to be severe at values of the chemical potential near a complex zero of the (unrooted) staggered determinant, which dictates the branch point sinularities of the complex square root function. At zero temperature, this is expected to happen for light-quark chemical potentials $\mu_q = \frac{\mu_B}{3} \gtrsim \frac{m_\pi}{2}$ [5]. See Fig. 1 for an illustration at a temperature in the confined phase. The purpose of this work is to study how thermodynamic observables are affected by these singularities.

2. Rooted staggered quarks at finite μ_B

In this study, we discuss the $2+1$-flavor theory in which a chemical potential is only introduced for degenerate light quarks and not for the strange quark. The phase reweighting scheme is adopted. The partition function of the phase-quenched ensemble reads:

$$\mathcal{Z}_{2+1}^{PQ}(T,\mu_q) = \int \mathcal{D}U |\det M^{1/2}(U,m_u,\mu_q)| \det M^{1/4}(U,m_s,0) e^{-S_{\rm YM}(U)}, \tag{1}$$

and is identical to the partition function with a finite isospin chemical potential, with $\mu_q = \mu_u = -\mu_d$. The partition function at finite baryochemical potential is obtained from the phase-quenched ensemble as

$$\frac{\mathcal{Z}_{2+1}}{\mathcal{Z}_{2+1}^{PQ}} = \left\langle \frac{\det M^{1/2}(U,m_u,\mu_q)}{|\det M^{1/2}(U,m_u,\mu_q)|} \right\rangle_{PQ}, \tag{2}$$

where $\langle \dots \rangle_{PQ}$ denotes the expectation value in the phase-quenched theory, defined by Eq. (1). Details of the method are explained in Ref. [7]. The prescription for rooting used here is to demand the determinant to be a continuous function of the chemical potential along the real axis [8].

3. A rise in the density at $\mu_B \gtrsim 3m_\pi/2$

We have recently shown that for the equation of state of the quark gluon plasma in the range $\mu_B/T \leq 3$, reweighting gives compatible results with analytic continuation from purely imaginary chemical potentials [9]. Thus, in the currently experimentally accessible range (the range of the RHIC Beam Energy Scan, phase two) the equation of state of the quark-gluon plasma is under control. The lowest temperature studied in Ref. [9] was 145 MeV. In an attempt extending these reweighting studies to lower temperatures, a sharp rise in the density as a function of the chemical potential at around $\mu_B = 3m_\pi/2$ is observed, as shown for a temperature of $T = 130$ MeV in Fig. 1. Such strong deviation of the reweighted results from the Taylor expansion in Fig. 1 prompts for cross-checks. To show that this effect is not the manifestation of the overlap problem of the reweighting procedure we reproduced the same result wuth the sign and phase reweighting schemes that are free from the overlap problem.

4. The four-flavor theory

If the observed sharp rise in the quark density is due to staggered rooting, it should be absent in the four-flavor theory in which all flavors of fermions have degenerate quark mass m and at identical chemical potentials $\mu_1 = \mu_2 = \mu_3 = \mu_4 = \mu_q$. The results can be contrasted with that of the same theory with two of the chemical potentials set at 0. The latter requires rooting and the sharp rise should occur, if rooting is the cause. Fig. 2 shows such comparison with a simulation at a pion mass of $m_\pi = 260$ MeV, a temperature $T = 100$ MeV and a lattice volume of $12^3 \times 8$. The scale was set using the w_0 scale of Ref. [10]. In the four-flavor case the Taylor expansion and the full reweighting match within errors. In the case of $\mu_1 = \mu_2 = \mu_q$ with $\mu_3 = \mu_4 = 0$, the reweighted curve rises sharply near $\mu_q = m_\pi/2$, and there is a very clear deviation between the Taylor and reweighted curves, resembling the sharp rise in the quark density that we observed in the 2 + 1-flavor case. The statistical errors for the (unrooted) four-flavor case are admittedly large at large μ_q. The error grows large precisely at the chemical potential where the rooted case takes a sharp turn, indicating large cancellations. Note that the four-flavor theory is expected to be noisier then the two-flavour

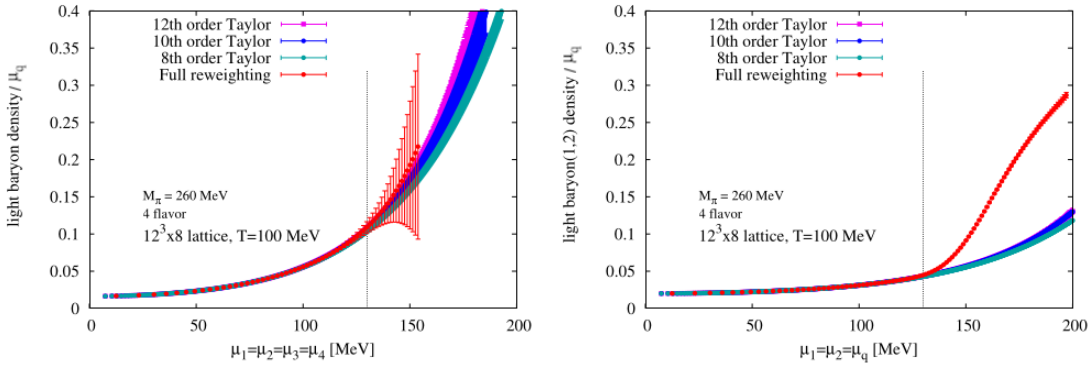

Figure 2: The density to chemical potential ratio for four flavors of quarks. Left: all quarks having the same chemical potential (this choice requires no rooting) Right: the chemical potential is introduced only for two of the four flavors, while the other two flavors remain at zero chemical potential (this choice requires rooting). Both cases where calculated using the same $\mu_q = 0$ ensemble. The vertical line corresponds to $\mu_q = m_\pi/2$.

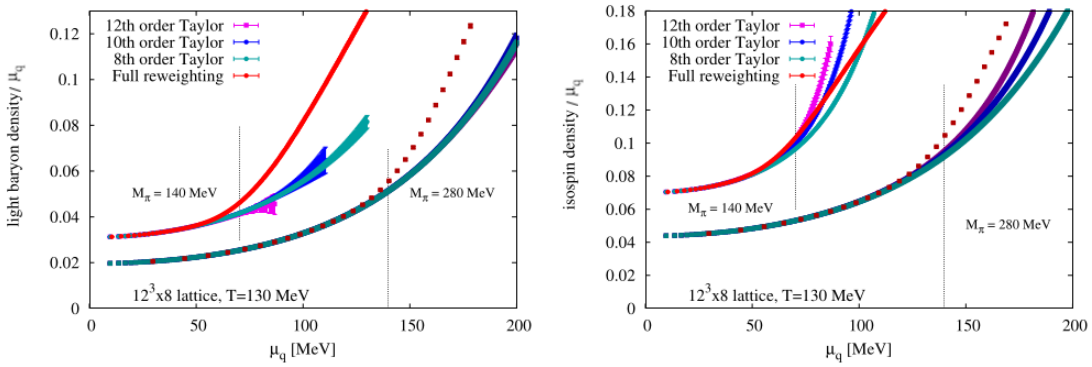

Figure 3: The full reweighted results for the light-quark density compared with several high orders of the Taylor expansion for the case of a baryon (left) and isospin (right) chemical potential for two different values of the pion mass. While the density itself looks very similar in the two cases, with a rapid rise for $\mu_q \gtrsim m_\pi/2$, the two singularities appear to be very different: At a finite isospin chemical potential - where the singularity of the free energy is due to a true phase transition - the Taylor expansion converges to the full reweighting result below $\mu_q \approx m_\pi/2$, and diverges above. On the other hand, at a finite baryon chemical potential, the Taylor expansion appears to converge, but above $\mu_q \approx m_\pi/2$ it converges to a different curve than the full reweighting one. This hints at a very different analytic structure.

theory, since the exponential severity of the sign problem has a factor of N_f^2 in the exponent [7], i.e. $\log \frac{\mathcal{Z}_{N_f}}{\mathcal{Z}_{N_f}^{PQ}} \propto N_f^2$. These findings are in line with our assumption that the sharp rise in the light-quark density for $\mu_B \gtrsim 3m_\pi/2$ is caused by staggered rooting.

5. Analytic structure and pion mass dependence

The observed rise looks similar to the way the isospin density behaves at the pion condensation transition [11], a transition that happens in the phase-quenched theory around the same value

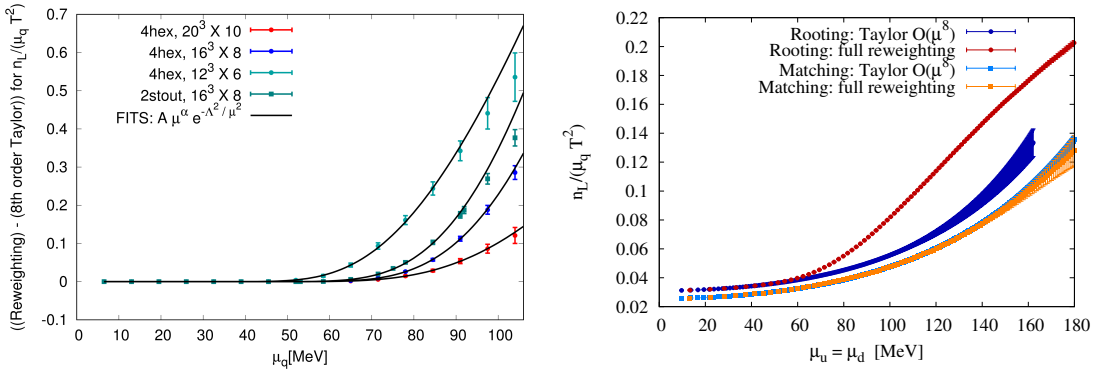

Figure 4: Left: The difference between the full reweighted result and the 8th-order Taylor expansion (which is assumed to be a good proxy for the analytic part of the density) for the light-quark density in units of the dimensionless quark chemical potential for the 4HEX action with 6,8 and 10 timeslices respectively. For comparison, results with the 2stout action with 8 timeslices are also shown. We also show fits of the form $A\mu_q^\alpha e^{-\Lambda^2/\mu_q^2}$. The fits were performed in the chemical potential range up to 85 MeV. Right: Geometric matching vs standard rooting on the $12^3 \times 8$ 2stout ensemble at a temperature $T = 130$ MeV. We show both full reweighting and Taylor expansion results. The sharp rise around $\mu_q = m_\pi/2$ is not observed with the geometric matching procedure.

$\mu_q = m_\pi/2$ of the quark chemical potential. The difference or similarity in analytic structure between the two is studied in Fig. 3. We performed high statistics simulations on $12^3 \times 8$ lattices with the 2stout action at physical quark mass and at four times physical quark mass, and measured Taylor coefficients of the pressure to 12th order in the chemical potential in both scenarios. For the case of an isospin chemical potential the rapid rise in the density is due to a second order phase transition [12] at $\mu_q \approx m_\pi/2$. At orders up to 12th, the Taylor expansion should converge to the full result until the transition point, above which it should diverge. This is exactly what is seen in the right panel of Fig. 3, at both of the simulated pion masses. The one important difference is that for the larger pion mass, the Taylor expansion seems to converge more slowly. This is not surprising, as the expansion parameter is μ_q/T, which is larger at the transition point for a heavier pion. Such divergent behavior is typical for phase transitions. It is very different from the behavior we observe at nonzero baryon density, seen in the left panel of Fig. 3. Here, the Taylor expansion appears to converge, but it converges to a different curve from the one obtained with full reweighting. Let us emphasize that the Taylor coefficients and the reweighting curve were obtained using the same gauge ensembles, and so the Taylor coefficients are exactly the Taylor coefficients of the reweighted curve at $\mu_q = 0$. Also note that while the point of divergence between the reweighting and Taylor curves does seem to scale with the pion mass, the two curves actually start to diverge already somewhat below $\mu_q = m_\pi/2$. This points to quite different non-analytic behavior, compared to the case of a nonzero isospin density. The singularity responsible for the behavior is likely an essential singularity. Details can be found in Ref. [1].

6. Continuum scaling with an action with strongly suppressed taste breaking

A natural question that arises is whether the observed non-analytic behavior of the free energy of rooted staggered fermions vanishes in the continuum limit, or not. To study this question, we

used a discretization with strongly suppressed taste breaking: the DBW2 gauge action and 4 steps of hex smearing, which we will call the 4HEX action. For this simulation we used physical quark masses at temperature $T = 130$ MeV, an aspect ratio $LT = 2$, and three different lattice spacings corresponding to $N_\tau = 6, 8$ and 10 time-slices each. In Fig. 4 we show the difference between full reweighting and an 8th-order Taylor expansion for the ratio $\hat{n}_L/\hat{\mu}$. For comparison, we also show results with the 2stout action at $N_\tau = 8$. One can see that the magnitude of the difference decreases rapidly with the lattice spacing. We did not manage to find a good fit ansatz to extrapolate this difference to the continuum, however. In particular, we do not observe the $O(a)$ scaling which is the expectation from the naive counting argument given in [3]. This might be due to the coarsest lattice ($N_\tau = 6$) being too coarse for seeing the asymptotic behavior. Notice, however, that if one assumes that the difference extrapolates to zero, then the observed decrease is not slower than the expected $O(a)$, but faster: rescaling the $N_\tau = 8$ data by a factor of $8/10$ gives numbers that are significantly above the lattice data at $N_\tau = 10$. Even rescaling the $N_\tau = 8$ data by $(8/10)^2$, the data on the $N_\tau = 10$ lattices is significantly below. Comparison with the 2stout results shows that at the same number of timeslices, the 4HEX action has a smaller non-analytic term. This is consistent with the expectation that reduced taste breaking (and thus the splitting of the taste multiplets in the spectrum) reduces this non-physical effect in the quark density.

7. Conclusion

We have shown that at nonzero baryochemical potential with rooted staggered fermions, where rooting ambiguity exists, the prescription of requiring continuity for the real values of chemical potential leads to a non-analytic contribution in the free energy. It manifests itself as a rapid rise of the light-quark density at low temperatures and baryochemical potential $\mu_B = 3\mu_q \gtrsim 3m_\pi/2$. This is at the same values of the quark chemical potential μ_q where the phase-quenched ensemble has a pion condensation transition. We showed that the non-analyticity is very different from a true thermodynamic phase transition by comparing with the case of an isospin chemical potential.Although the behavior of the light-quark density as a function of the chemical potential looks very similar in the two cases, the phase transition at nonzero isospin density leads to a branch-point singularity at some nonzero μ, while rooting leads to an essential singularity at $\mu_B = 0$. There are several possible approaches to resolve this issue. An example is geometric matching that identifies eigenpairs and replaces them with their geometric mean [4]. Another is to adopt a different discretization formulation other than staggered, such as the Karsten-Wilczek formulation[13, 14] .

8. Acknowledgements

The project was supported by the BMBF Grant No. 05P21PXFCA. This work is also supported by the MKW NRW under the funding code NW21-024-A. Further funding was received from the DFG under the Project No. 496127839. This work was also supported by the Hungarian National Research, Development and Innovation Office, NKFIH Grant No. KKP126769. This work was also supported by the NKFIH excellence grant TKP2021_NKTA_64. The authors gratefully acknowledge the Gauss Centre for Supercomputing e.V. (www.gauss-centre.eu) for funding this project by providing computing time on the GCS Supercomputers Jureca/Juwels [15] at Juelich Supercomputer Centre and HAWK at Höchstleistungsrechenzentrum Stuttgart.

References

[1] S. Borsanyi, Z. Fodor, M. Giordano, J.N. Guenther, S.D. Katz, A. Pasztor et al., *Can rooted staggered fermions describe nonzero baryon density at low temperatures?*, 2308.06105.

[2] A. Pasztor, *Lattice QCD Overview*, *Quark Matter Proceeding* (2023) .

[3] M. Golterman, Y. Shamir and B. Svetitsky, *Breakdown of staggered fermions at nonzero chemical potential*, *Phys. Rev. D* **74** (2006) 071501 [hep-lat/0602026].

[4] M. Giordano, K. Kapas, S.D. Katz, D. Nogradi and A. Pasztor, *Radius of convergence in lattice QCD at finite μ_B with rooted staggered fermions*, *Phys. Rev. D* **101** (2020) 074511 [1911.00043].

[5] Z. Fodor, K.K. Szabo and B.C. Toth, *Hadron spectroscopy from canonical partition functions*, *JHEP* **08** (2007) 092 [0704.2382].

[6] A. Hasenfratz and D. Toussaint, *Canonical ensembles and nonzero density quantum chromodynamics*, *Nucl. Phys. B* **371** (1992) 539.

[7] S. Borsanyi, Z. Fodor, M. Giordano, S.D. Katz, D. Nogradi, A. Pasztor et al., *Lattice simulations of the QCD chiral transition at real baryon density*, *Phys. Rev. D* **105** (2022) L051506 [2108.09213].

[8] Z. Fodor and S.D. Katz, *Critical point of QCD at finite T and mu, lattice results for physical quark masses*, *JHEP* **04** (2004) 050 [hep-lat/0402006].

[9] S. Borsanyi, Z. Fodor, M. Giordano, J.N. Guenther, S.D. Katz, A. Pasztor et al., *Equation of state of a hot-and-dense quark gluon plasma: Lattice simulations at real μB vs extrapolations*, *Phys. Rev. D* **107** (2023) L091503 [2208.05398].

[10] BMW collaboration, *High-precision scale setting in lattice QCD*, *JHEP* **09** (2012) 010 [1203.4469].

[11] B.B. Brandt and G. Endrodi, *Reliability of Taylor expansions in QCD*, *Phys. Rev. D* **99** (2019) 014518 [1810.11045].

[12] D.T. Son and M.A. Stephanov, *QCD at finite isospin density*, *Phys. Rev. Lett.* **86** (2001) 592 [hep-ph/0005225].

[13] L.H. Karsten, *Lattice Fermions in Euclidean Space-time*, *Phys. Lett. B* **104** (1981) 315.

[14] F. Wilczek, *ON LATTICE FERMIONS*, *Phys. Rev. Lett.* **59** (1987) 2397.

[15] D. Alvarez, *JUWELS cluster and booster: Exascale pathfinder with modular supercomputing architecture at juelich supercomputing centre*, *Journal of large-scale research facilities JLSRF* **7** (2021) .

PoS(LATTICE2023)166